4th GRACM Congress on Computational Mechanics
GRACM 2002
Patra, 27-29 June, 2002

A COMPARATIVE STUDY BETWEEN COONS-PATCH MACROELEMENTS AND BOUNDARY ELEMENTS IN TWO-DIMENSIONAL POTENTIAL PROBLEMS

Christopher G. Provatidis

Laboratory of Dynamics and Mechanical Structures
National Technical University of Athens
157 73 Athens, Greece
e-mail: cprovat@central.ntua.gr

Keywords: Boundary Elements, Coons patch, Finite Elements, Macroelements, Potential Problems.

Abstract. *This paper discusses a recently appeared method, which is here called "Coons-patch"-macroelement approach, where degrees of freedom appear at the boundaries only. This method is compared with the well-known Boundary Element Method for the same nodal points on the boundary. The comparison refers to both static (Laplace) and eigenvalue two-dimensional potential problems with straight and curvilinear boundaries in three characteristic examples with known analytical closed solutions.*

1 INTRODUCTION

Most engineering boundary-value problems are usually solved by either the Finite Element Method (FEM)[1] or the Boundary Element Method (BEM)[2]. The advantage of the FEM lies on the fact that it is easily applicable to all type of problems but it suffers from the mesh generation task. On the contrary, the application of the BEM requires the discretization of only the boundary and it is capable of solving linear problems as well as nonlinear ones, where, sometimes, internal cells are considered and associated domain integration is performed. In general, BEM is characterized by fully-occupied and nonsymmetric matrices that can be also properly symmetrized [3].

In case of dynamic analysis, the FEM requires two *constant* matrices (mass matrix **M**, stiffness matrix **K**), while the BEM requires two *frequency-dependent* matrices (**H** and **G**). The latter disadvantage of the BEM led to the alternative Dual Reciprocity Method (DRM) [4]. Within the last twenty years, a lot of authors [2,5-7] have claimed that DRM works satisfactorily but in acoustic eigenvalue problems a different opinion prevails [8-13].

In this context, a question arises whether it may be possible to construct a class of new large elements that are sufficiently accurate in static analysis as well as in eigenvalue acoustic analysis. In both cases the objective is to reduce the time of data preparation task. From a general point of view, macro-elements that straightly use global cardinal shape functions may be introduced. Generally, between the possibilities of constructing such functions, one may choose to fulfil the homogeneous partial differential equation (PDE) or alternatively only the boundary conditions and not the PDE. Moreover, it is possible to fulfil both the PDE and the boundary conditions, as shown by Provatidis and Kanarachos [3] some years ago. From the practical point of view, the disadvantage of applying global shape functions fulfilling the PDE is the fact that these fail to reproduce eigenmodes. For example, in the case of the wave-propagation equation in a rectangular acoustical cavity, harmonic global functions, which in other words fulfil *Laplace*'s equation, are not capable of approximating the well-known non-harmonic sinusoidal modes, excepting the case of introducing internal degrees of freedom [8-15].

In the context of fulfilling the boundary conditions only, the use of large finite-elements based on *Coons-Patch* (**CP**) interpolation theory [16], with degrees of freedom appearing only at the element boundaries has appeared in two-dimensional and axisymmetric potential and elasticity problems [17-21]. Up to now, this method was found to have excellent behaviour in both static and dynamic problems.

This paper extends the theory of the CP-elements and it further investigates its accuracy in comparison to the BEM in typical static and dynamic examples where advantages and disadvantages of both methods are shown.

2 GENERAL THEORY

Two-dimensional potential problems mainly include:

i) Laplace equation

$$\nabla^2 u = \frac{\partial^2 u}{\partial x^2} + \frac{\partial^2 u}{\partial y^2} = 0 \tag{1}$$

and also

ii) Wave propagation equation

$$\left(\frac{1}{c^2}\right)\frac{\partial^2 u}{\partial t^2} - \left(\frac{\partial^2 u}{\partial x^2} + \frac{\partial^2 u}{\partial y^2}\right) = 0 \tag{2}$$

The boundary conditions are:

$$\begin{aligned} u &= u_\Gamma(t) \text{ on } \Gamma_1 \\ q &= q_\Gamma(t) \text{ on } \Gamma_2 \end{aligned} \tag{3}$$

In (1), (2) and (3) u denotes the potential, $q = \partial u / \partial n$ the flux (n=outward unit normal vector), c the velocity of the wave propagation, ∇ the Nabla operator, t the time, and Γ_1 and Γ_2 parts of the boundary Γ where the potential and the flux, respectively, is prescribed (Figure 1).

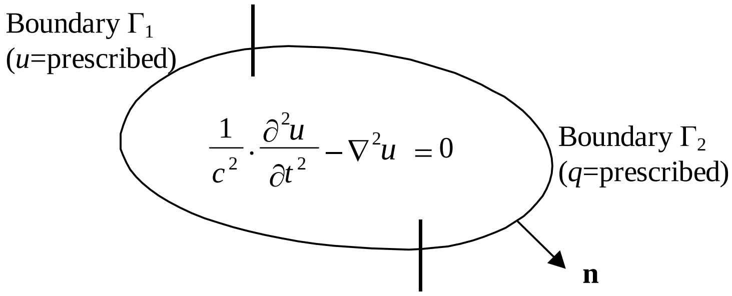

Figure 1. Problem domain and boundary conditions

The problem domain is considered as a four-sided patch in the (x,y)-plane. This patch is mapped to a reference patch (ξ,η), where the normalized curvilinear coordinates are ($0 \le \xi, \eta \le 1$) as shown in Figure 2.

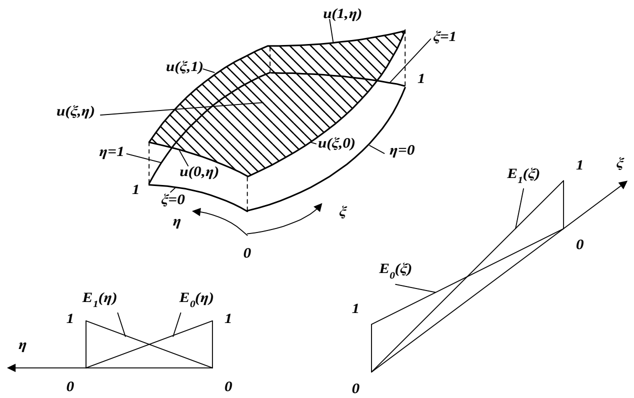

Figure 2. Reference Coons patch

According to Coons' interpolation formula [16], each point $\mathbf{x}(\xi,\eta)=\{x(\xi, \eta), y(\xi, \eta)\}^T$ along the patch can be approximated by its boundaries $\left(\mathbf{x}(\xi,0), \mathbf{x}(\xi,1), \mathbf{x}(0,\eta), \mathbf{x}(1,\eta)\right)$ as follows (see also [20]):

$$\begin{aligned} \mathbf{x}(\xi,\eta) = {} & E_0(\xi)\mathbf{x}(0,\eta) + E_1(\xi)\mathbf{x}(1,\eta) + E_0(\eta)\mathbf{x}(\xi,0) + E_1(\eta)\mathbf{x}(\xi,1) - E_0(\xi)E_0(\eta)\mathbf{x}(0,0) \\ & - E_1(\xi)E_0(\eta)\mathbf{x}(1,0) - E_0(\xi)E_1(\eta)\mathbf{x}(0,1) - E_1(\xi)E_1(\eta)\mathbf{x}(1,1) \end{aligned} \tag{4}$$

where for C^0-continuity discrete problems the blending functions are linear and equal to:

$$\begin{aligned} E_0(\xi) &= 1-\xi \ , \quad E_1(\xi) = \xi \\ E_0(\eta) &= 1-\eta \ , \quad E_1(\eta) = \eta \end{aligned} \tag{5}$$

Following the idea of isoparametric elements [1], equation (4) is extended from the geometrical quantities $\mathbf{x}(x,y)$

to the interpolation of the potential $u(\xi,\eta)$, as follows.

$$\begin{aligned} u(\xi,\eta) = {} & E_0(\xi)u(0,\eta) + E_1(\xi)u(1,\eta) + E_0(\eta)u(\xi,0) + E_1(\eta)u(\xi,1) \\ & - E_0(\xi)E_0(\eta)u(0,0) - E_1(\xi)E_0(\eta)u(1,0) \\ & - E_0(\xi)E_1(\eta)u(0,1) - E_1(\xi)E_1(\eta)u(1,1) \end{aligned} \tag{6}$$

If the boundary values $u(\xi,0)$, $u(\xi,1)$, $u(0,\eta)$ and $u(1,\eta)$ are interpolated by any set of trial functions, and then equation (5) is collocated to all boundary nodes, inside the reference macro-element, the solution $u(\xi,\eta)$ is approximated by:

$$u(\xi,\eta) = \sum_{k=1}^{N_e} N_k(\xi,\eta)\, u_k(t), \tag{7}$$

with $u_k(t)$ denoting nodal degrees of freedom appearing only at the boundaries of the macro-element, N_e the total number of the nodes along that and $N_k(\xi,\eta)$ the global shape functions. In the particular choice that trial functions is to use cubic B-splines, $N_k(\xi,\eta)$ are given as [21]:

i) Corner nodes:

$$\begin{aligned} N_A(\xi,\eta) &= E_0(\xi)B_{q_4}^{(4)}(\eta) + E_0(\eta)B_1^{(1)}(\xi) - E_0(\xi)E_0(\eta) \\ N_B(\xi,\eta) &= E_1(\xi)B_1^{(2)}(\eta) + E_0(\eta)B_{q_1}^{(1)}(\xi) - E_1(\xi)E_0(\eta) \\ N_C(\xi,\eta) &= E_1(\xi)B_{q_2}^{(2)}(\eta) + E_1(\eta)B_1^{(3)}(\xi) - E_1(\xi)E_1(\eta) \\ N_D(\xi,\eta) &= E_0(\xi)B_1^{(4)}(\eta) + E_1(\eta)B_{q_3}^{(3)}(\xi) - E_0(\xi)E_1(\eta) \end{aligned} \tag{8}$$

ii) Interior nodes to AB: $N_j(\xi,\eta) = E_0(\eta)B_j^{(1)}(\xi)\ ,\ 2 \le j \le q_1 - 1$ (9)

iii) Interior nodes to BC: $N_j(\xi,\eta) = E_1(\xi)B_j^{(2)}(\eta)\ ,\ 2 \le j \le q_2 - 1$ (10)

iv) Interior nodes to CD: $N_j(\xi,\eta) = E_1(\eta)B_j^{(3)}(\xi)\ ,\ 2 \le j \le q_3 - 1$ (11)

v) Interior nodes to DA: $N_j(\xi,\eta) = E_0(\xi)B_j^{(4)}(\eta)\ ,\ 2 \le j \le q_4 - 1$ (12)

Typical global shape functions for a rectangular macro-element of fifty nodes may be found in References [18-21]. Again, these are cardinal functions ([1-0]-type), as it happens in the case of conventional Lagrangian or Serendipity finite elements (definitions may be found for example in Ref.[1]).

3 INTERNAL POINTS

To each couple of natural co-ordinates (ξ,η) the corresponding couple of Cartesian ones (x,y) is found in a straight way through Eq.(4). On the contrary, when the potential at an internal point (x_i, y_i) is requested, then the corresponding couple of natural co-ordinates (ξ_i,η_i) have to be found by trial-and-error (nonlinear procedure). In simple rectangular domains the (ξ_i,η_i)s can be easily determined by inspection or minor calculations even by hand. However, in case of more complicated curvilinear domains (circle, ellipse, et cetera) a simple iterative scheme such as Newton-Raphson is required. Then, the potential is calculated on the basis of boundary values and global shape functions using Eq.(7). Obviously, the calculation of the global shape functions that correspond to each internal point is a trivial task. A similar procedure is followed for the internal fluxes by differentiating Eq.(7).

4 EXAMPLES

The accuracy of the proposed CP-macroelements will be elucidated through three test cases where analytical solutions are known. Comparison is performed with linear and quadratic boundary elements with the same number of boundary nodes.

4.1 Example 1: Singular temperature in rectangular adiabatic plate

This example was taken from [3,17] and refers to a thin rectangular plate free of heat sources, insulated at the top and bottom surfaces with dimensions L=2a=6 and b=12 (Figure 3). The analytical solution is given as

$$T(x,y) = T_m\left[\sinh\left(\pi y/L\right)\Big/\sinh\left(\pi b/L\right)\right]\cos\left(\pi x/L\right) \tag{13}$$

with the temperature T_m being equal to T_m=100°C. Obviously, the above exact solution is a very steep exponential function along the y-axis of symmetry. Due to the symmetry of the problem with respect to the y-axis, only half the domain is to be analyzed.

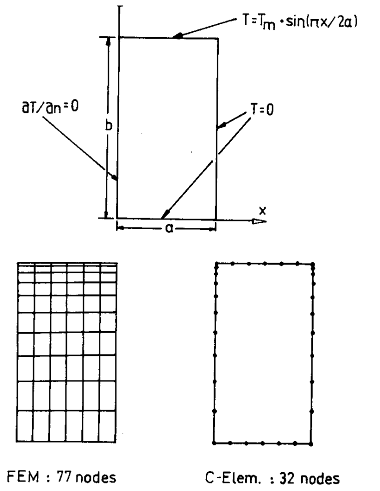

Figure 3. Rectangular adiabatic plate

The problem is analyzed using FEM, BEM and CP-macroelements and the same *non-uniform* mesh on the boundary. In the last case, two different options are considered. The first option was previously applied in Ref.[17] and it is characterized by linear blending functions in both directions according to Eq.(5).

The second option is applied in this paper for first time and it is characterized by linear blending functions in *y*-direction (eq.(5)) and *sinusoidal* ones in *x*-direction:

$$E_0(\xi)=\cos\left(\frac{\pi\xi}{2}\right)\ ,\quad E_1(\xi)=1-\cos\left(\frac{\pi\xi}{2}\right) \qquad (14)$$
$$E_0(\eta)=1-\eta\ ,\quad E_1(\eta)=\eta$$

Despite the fact that the linear blending functions are not sufficient to sufficiently approximate the solution, the sinusoidal ones *dramatically* reduce the numerical error as shown in Table 1 (shadowed bottom area: mean average error=0.52%). Obviously, this occurs because the sinusoidal blending function accurately approximates the sinusoidal boundary condition on the top of the plate.

Table 1: Temperature distribution in a rectangular adiabatic plate with *L*=6 (*L*=2*a*) and *b*=12. Comparison between the 32-node CP-element with the FEM(77-node four-node bilinear elements) and the BEM (32-nodes).

y	Exact Solution	Errors in %			
		FEM 77 DOF	BEM 32 DOF	Macro-element 32-DOF Ref.[17, p.105]	CP-element 32-DOF **Present paper**
12.000	100.0000	Data	Data	Data	Data
11.781	89.2034	0.09	0.32	0.34	-0.024
11.345	70.9852	0.32	0.40	0.84	-0.004
10.691	50.3861	0.75	0.49	3.08	+0.047
9.818	31.9046	1.51	0.68	6.33	+0.093
8.727	18.0200	2.73	1.04	10.00	+0.172
7.418	9.0768	4.59	1.77	13.80	+0.363
5.891	4.0729	7.29	3.25	16.58	+0.692
4.145	1.6152	10.91	6.30	16.65	+1.237
2.182	0.5257	14.97	12.95	10.00	+2.073
0.	0.	Data	Data	Data	Data
Mean average absolute error (%)		4.80	3.02	8.62	**0.52**

4.2 Example 2: Elliptic bar under tension

This example refers to an elliptical bar under torsion (Laplace equation) shown in Figure 4. Suppose that a uniform isotropic rod is fixed at one end, and that any section of the rod at distance *z* from the fixed end is twisted through an angle θz, so that θ is the angle of twist per unit length. The displacement *w* in the direction of *z*-axis is independent of *z*. Under Saint-Venant type torsion the displacements are given by [22,23]:

$$u = -\theta\, y\, z,\; v = +\theta\, x\, z,\; w = +\theta\, \phi \tag{15}$$

where θ is the torsion angle per unit length and $\phi(x, y)$ is the warping function given by

$$\nabla^2 \phi = 0 \tag{16}$$

In the particular case of an elliptic section, the analytical solution of Eq.(16) is given by

$$\phi = -\frac{\left(a^2 - b^2\right)}{a^2 + b^2} x y \tag{17}$$

The boundary conditions refer to tractions normal to the boundary that are identically zero, hence

$$\frac{\partial \phi}{\partial n} = |r| \cos(\vec{r}, \vec{t}) \tag{18}$$

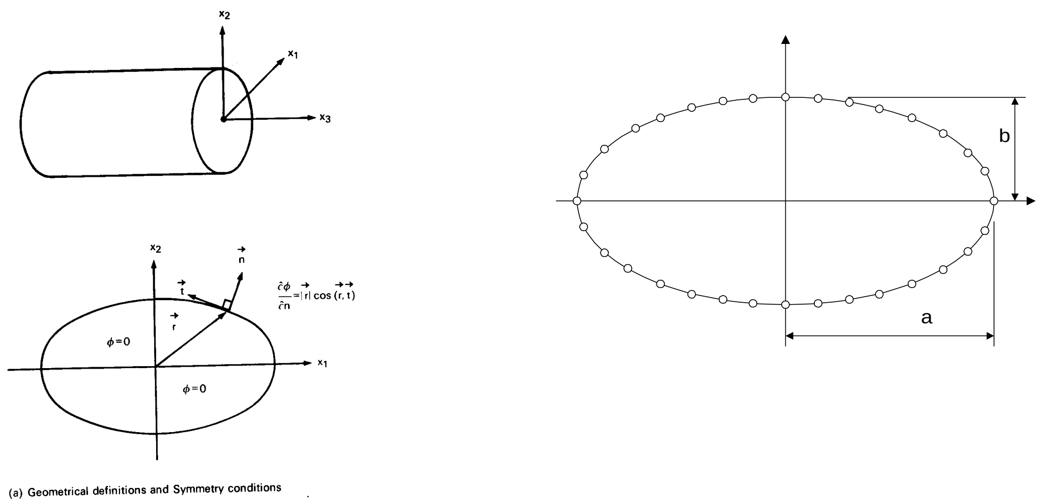

Figure 4. Elliptical section in torsion

For the case of an ellipse this becomes,

$$\frac{\partial \phi}{\partial n} = \frac{a^2 - b^2}{\sqrt{a^4 y^2 + b^4 x^2}} x\, y \tag{19}$$

Since for all interior problems *Neumann* boundary conditions do not insure the *uniqueness* of the solution, the nodal point at ($x = a, y = 0$) was assigned a zero value.

The dimensions were assumed to be *a*=10 and *b*=5 and values of ϕ on the boundary and at two selected internal points $(x = 2, y = 2)$ and $(x = 4, y = 3.5)$ were computed.

The boundary was divided into thirty-two nodal points, which also define (Figure 4):

- One CP-macroelement
- Thirty-two linear boundary elements or
- Sixteen quadratic boundary elements.

Results for some representative boundary nodes and two internal points are compared with the known exact solution in Table 2. It is noted that the natural (ξ,η) co-ordinates for the above mentioned two internal points are (0.566,0.284) and (0.580,0.101), respectively. As was explained in Section 3, these were found using the Newton-Raphson method.

Table 2: Calculated potentials at representative boundary and internal nodes using the proposed Coons-patch B-splines method and conventional (linear, quadratic) boundary elements.

Boundary node	Coons-patch macroelement	Boundary elements		Exact potential solution
		Linear	Quadratic	
$x_1 = 8.814$, $x_2 = 2.361$	-12.437	-12.412	-12.506	-12.489
$x_1 = 6.174$, $x_2 = 3.933$	-14.703	-14.501	-14.576	-14.570
$x_1 = 3.304$, $x_2 = 4.719$	-9.276	-9.34	-9.363	-9.356
Internal points				
$x_1 = 2.$, $x_2 = 2.$	-2.371	-2.399		-2.400
$x_1 = 4.$, $x_2 = 3.5$	-8.358	-8.402		8.400

The mean average value of absolute errors for the proposed and BEM is 0.95% and 0.24%, respectively. In other words, in this particular problem the proposed CP-element is less accurate.

4.3 Example 3: Circular acoustic cavity

The last example refers to a circular acoustic cavity of unit radius $(a=1)$ with Neumann $(\partial u/\partial n = 0)$ boundary conditions and velocity c=1m/s and exact eigenvalues given as $J'_m(ka)=0$, $m=0,1,2,\ldots$ where $J'_m(ka)$ is the derivative of the Bessel function of first kind of order m and $k=\omega/c$ the wavenumber.

In the beginning, the boundary of the circle was uniformly divided into thirty-two boundary segments with equal number of nodal points. These points alternatively define:

- One 32-noded Coons patch macroelement
- Thirty-two constant boundary elements or
- Thirty-two linear boundary elements

The following analysis includes two types of mass matrices, i.e. consistent and lumped ones.

I. Consistent mass matrices were obtained in a similar way as in [15], based on the standard Nardini-Brebbia mass $\mathbf{M}_{\boldsymbol{\alpha}}$ [4], which leads to the final mass $\mathbf{M} = \mathbf{L}\,\mathbf{G}^{-1}\mathbf{M}_a\,\mathbf{F}^{-1}$ and the equivalent stiffness matrix $\mathbf{K}_{eq} = \mathbf{L}\,\mathbf{G}^{-1}\,\mathbf{H}$.

As it is shown in Table 3, the proposed Coons-patch macroelements are sufficiently accurate while the BEM-solution using *boundary-only* conical base functions (DRM: Nardini-Brebbia) is not capable of approximating upper modes. It is noted that the superiority of the CP-macroelement is here less clear than what it had been found in Reference [17] for the case of a rectangular cavity.

Moreover, it is noted that the BEM-based mass matrix *does not preserve (exceeds) the area of the circle*, i.e. the sum of all elements of mass matrix (properly multiplied) differs than the total mass of the circle. Results were obtained for N=16,32,64 and 128 boundary nodes. It is remarkable that although the discretized domain is a polygon *inscribed* to the circle, it has a *smaller* area that what the circle has (3.1415926), even for a small number of boundary nodes the calculated mass is larger and it hardly converges to the correct value. A similar result has been found earlier for a rectangular cavity [10].

Table 3: Coons-patch macroelement and BEM solution with *consistent* masses for a circular acoustical cavity of unit radius, c=1m/s and N_b=32 nodal points (Neumann boundary conditions).

EXACT EIGENVALUES	CALCULATED EIGENVALUES			
	CP-macroelement		Boundary Elements	
	Linear	B-Splines	Constant	Linear
$\omega_1^2 = 0.000$	0.000	0.000	0.000	0.000
$\omega_2^2 = \omega_3^2 = 3.390$	3.570	3.531	3.833	3.836
$\omega_4^2 = \omega_5^2 = 9.328$	10.057	9.676	10.354	10.472
$\omega_6^2 = 14.682$	19.359	18.041	20.563	20.760
$\omega_7^2 = \omega_8^2 = 17.650$	20.921	19.691	34.340	34.648
$\omega_9^2 = \omega_{10}^2 = 28.277$	34.421	31.623	52.237	52.640

II. Lumped mass matrices were also studied. As shown in Reference [15], a study concerning acoustical cavities, the BEM is not capable to handle lumped masses located on the boundary. On the contrary, when these lumped masses are distributed within the domain, then BEM achieves to accurately solve the algebraic eigenvalue problem. Similar observations were made in elastodynamics of plates [24].

In Reference [15] there were made three attempts to develop BEM lumped masses, as follows:

(a) Equivalent stiffness matrix $\mathbf{K}_{eq} = \mathbf{L}\mathbf{G}^{-1}\mathbf{H}$ was combined with boundary lumped masses; each of them was equal to 1/32 of the total mass inside the circle ($\pi\times1^2$=3.14)

(b) Cardinal shale functions that satisfy the Laplace equation were used.

(c) Lumped masses on the boundary (each of them equal to π/32) were introduced into the partial differential equation, as Dirac inertia terms.

For the purposes of this paper a fourth attempt was made by adding all elements of the corresponding row in the consistent BEM mass, which was obtained through the radial basis $f_j = R$. It was validated that all these lumped masses were equal each other.

With respect to Coons-patch macroelements, two further attempts were made:

- Lumped masses were created by adding all elements in the corresponding row of consistent mass matrix. In this case, the masses at the corners (A,B,C and D) of the reference macroelement were found to be negative and the four lowest eigenvalues were also negative!
- Due to the geometrical symmetry of this particular problem, in analogy to the consistent matrix, only five lumped masses were considered as the explicit variables in a *minimization* problem with objective function $OBJ = \left(\omega_{1,calc}^2 - \omega_{1,exact}^2\right)^2$ and similar. Starting from the abovementioned "bad" initial value, both unconstrained (FMINUNC) and constrained (FMINCON) optimization algorithms in MATLAB 6.1 (Release 12.1) resulted in *equal* lumped masses!
- A summary of the new and older results are shown in Table 4.

Table 4: Calculated eigenvalues of the circular cavity using several formulations of *lumped* mass.

EXACT	**CP-macro**	**Nardini**	**Reference [15]**		
			(a)	**(b)**	**(c)**
0.000	0.000	0.000	0.000	0.000	0.000
3.390	2.000	1.897	2.013	1.987	2.028
9.328	3.936	3.829	4.062	3.898	4.112
14.682	5.987	5.805	6.159	5.660	6.246
17.650	7.670	7.831	8.309	7.210	8.422
28.277	22.178	9.907	10.511	8.502	10.623

It can be there noticed that:

- All formulation fail to approximate even the first nonzero eigenvalue.
- All formulations lead to essentially similar results.

5 DISCUSSION - CONCLUSIONS

It was shown that the proposed Coons-patch macroelements are capable of accurately solving potential problems such as steady-state temperature distribution, torsion problems of beam sections, as well as natural frequencies of acoustical cavities. With respect to the BEM solution, it was found that:

1. In static problems, the proposed Coons-patch macroelement is competitive in accuracy with BEM. However, in its present form the method is not capable of dealing with internal holes and exterior domains.
2. In dynamic problems, the accuracy of the proposed method is superior to the BEM since it converges without requiring internal degrees of freedom. The method does not work in conjunction with lumped masses.

REFERENCES

[1] Bathe K.J. (1996), *Finite Element Procedures*, Prentice Hall, NJ.

[2] Brebbia C.A. and Dominguez, J. (1992), *Boundary Elements: An Introductory Course*, (Computational Mechanics Publications, McGraw-Hill Book Company).

[3] Kanarachos, A.E., Provatidis,C.G. (1988), “On the Symmetrization of the BEM formulation”, Comput. Methods Appl. Mech. Eng, Vol. 71, pp. 151-165.

[4] Nardini D., Brebbia C.A. (1982), A new approach to free vibration analysis using boundary elements, In: Brebbia C.A. (Ed.), Boundary Element Methods in Engineering, Proc. 4th Int. Seminar (Southampton, England), pp. 312-326, Berlin: Springer-Verlag.

[5] Nowak A.J. and Neves A.C. (1994), *The Multiple Reciprocity Boundary Element Method*, Southampton, U.K.: Computational Mechanics Publications.

[6] Beskos D.E. (1995), “Dynamic inelastic structural analysis by boundary element methods”, Archives of Computational Methods in Engineering, Vol. 2, pp. 1-33.

[7] Beskos D.E. (1997), “Boundary elements methods in dynamic analysis: Part II (1986-1996)”, Appl Mech Rev, Vol. 50, 149-197.

[8] Provatidis C.G. (1987), *On the application of the boundary element method in the analysis of field and dynamic problems*, Doctoral Dissertation, Department of Mechanical Engineering, National Technical University of Athens (in Greek).

[9] Kanarachos A.E., Provatidis C.G. (1987), “Performance of mass matrices for the BEM dynamic analysis of wave propagation problems”, Comput. Methods Appl. Mech. Eng., Vol. 63, pp. 155-165.

[10] Provatidis C.G., Kanarachos A.E. (1995), “Further research on the performance of consistent mass matrices using BEM for symmetric/nonsymmetric formulations”, Computational Mechanics, Vol. 16, pp. 197-205.

[11] Coyette J.P. and Fyfe K.R. (1990), “An improved formulation for acoustic eigenmode extraction from boundary element models”, J. Vibr. Acous. Trans. ASME, Vol. 112, pp. 392-398.

[12] Ali A., Rajakumar C. and Yunus S.M. (1991), “On the formulation of the acoustic boundary element eigenvalue problems”, Int J Numer Meth Engng, Vol. 31, pp. 1271-1282.

[13] Ali A., Rajakumar C. and Yunus S.M. (1995), “Advances in acoustic eigenvalue analysis using boundary element method”, Computers & Structures, Vol. 56, pp. 837-847.

[14] Kanarachos A.E., Provatidis C.G. (1992), “Potential and wave propagation problems using the Boundary Element Method and BEM-subregions”, Engineering Analysis with Boundary Elements, Vol. 9, pp. 117-124.

[15] Provatidis C.G., Kanarachos A.E. (1993), “On the BEM lumped mass formulations of wave equation problems”, Engineering Analysis with Boundary Elements, Vol. 11, pp. 319-325.

[16] Coons S.A. (1967), *Surfaces for computer aided design of space form*, Project MAC, MIT (1964), revised for MAC-TR-41. Springfield, VA, U.S.A.: Available by CFSTI, Sills Building, 5285 Port Royal Road.

[17] Kanarachos A. and Deriziotis D. (1989), “On the solution of Laplace and wave propagation problems using «C-elements»”, Finite Element in Analysis and Design, Vol. 5, pp. 97-109.

[18] Kanarachos A.E., Provatidis C.G., Deriziotis D., Foteas N., “A new approach of the fem analysis of two-dimensional elastic structures using global (Coons’s) interpolation functions”, ECCM’99 (CD Proceedings)

[19] Provatidis, C.G., Kanarachos, A.E. (2000), “On the use of Coons’ interpolation in CAD/CAE applications”, in: N.Mastorakis, ed., Systems and Control: Theory and Applications (World Scientific and Engineering Society Press, http://www.worldses.org), pp. 343-348.

[20] Provatidis C.G. and Kanarachos A.E. (2001), “Performance of a macro-FEM approach using global interpolation (Coons’) functions in axisymmetric potential problems”, Computers & Structures, Vol. 79,pp. 1769-1779.

[21] Provatidis C.G. (2002), “Analysis of axisymmetric structures using Coons interpolation”, Finite Elements in Analysis and Design (in press).

[22] Prescott J. (1961), *Applied Elasticity*, Dover Publications, New York.

[23] Katsikadelis J.T. (1999), *Boundary Elements in Engineering Science: Theory and applications*, Symeon Publ., Athens.

[24] Katsikadelis J.T. and Kandilas CB (1990), “Flexibility matrix solution of the vibration problem of plates based on the boundary element method”, Acta Mech, Vol. 83, pp. 51-60.